

A Topographic Gamut Mapping Algorithm Based on Experimental Observer Data

Lindsay MacDonald, Ján Morovic and Kaida Xiao
Colour & Imaging Institute, University of Derby, United Kingdom

Abstract

A new gamut mapping algorithm is proposed, based on analysis of observer preferences in a previous interactive gamut mapping experiment. The new algorithm preserves the colour relationships between the original and reproduced images, by matching the local conformations of the source and destination gamut boundaries. A core gamut is constructed inside the destination gamut boundary, within which no mapping occurs, i.e. colour is preserved unchanged. Colours outside the destination gamut are mapped into the region between the core and destination gamut boundaries in a reversible manner. Results of a first set of experiments are reported, with 12 observers, 5 images and 4 algorithms, indicating that the new algorithm performed well but that scope remains for further improvement.

Introduction

It remains a significant problem how best to reproduce the colours of an image that lie outside the colour gamut of a given device. There can be no single optimal method, because various conflicting demands must be taken into account:

- Achieve a specified reproduction objective or *rendering intent*;
- Make best use of the available colour gamut of the output device;
- Not introduce any visible artefacts, such as contouring, into the image;
- Minimise computational complexity for efficient processing.

Developments in colour imaging techniques over the past decade have separated the problem into three areas – device characteristics, colour appearance and gamut mapping – enabling each to be studied in greater detail. Gamut mapping algorithms (GMAs) in particular have steadily become more sophisticated since the crude 'clip to range limits' methods of early computer graphics. Studies by Morovic and Luo[1] and Braun *et al.*[2] have indicated that different algorithms are preferred by observers not only for different device colour gamuts, but also for different regions of colour space. Also the characteristics of individual images are crucial – generally much better results can be achieved by analysis of the distribution of colours within an image than by applying a generic algorithm.[3,4]

It is generally agreed that gamut mapping should be performed in a perceptually uniform colour space such as CIELAB or CIECAM97s.[5] This provides more control over the appearance of the image, and allows the techniques of Cartesian geometry to be applied to equally scaled dimensions of lightness, chroma and hue, in which one unit corresponds approximately to one just-noticeable difference (JND). The CIECAM97s colour model yields superior uniformity and independence of media and viewing conditions, although it is more complex to compute. Throughout this paper we shall assume that a uniform colour space is employed, and denote the lightness and chroma axes by L and C respectively.

Gamut Mapping Algorithms

Various methods of gamut compression have been proposed, from the basic clipping of colours to the nearest point on the gamut boundary to complex transformations of colour space in which the lightness, chroma and in some cases also hue are modified. The best results to date have been obtained by the CARISMA algorithm, first proposed by Johnson[6] and further developed by Morovic and Luo[1] and Green and Luo[7]. A recent evaluation by Pirrotta *et al.*[8] confirmed that it performs well for photographic images but not very well for business graphics and illustrations.

One of the problems with the majority of previous algorithms, is that they attempt to map all colours in the L-C plane (at constant hue) toward a single convergence point, or 'centre of gravity', based on the co-ordinates of the cusps (points of maximum chroma) of the original and reproduction gamuts. An example is the SLIN algorithm[1], in which colours are mapped toward the point L=50 on the lightness axis. Different rules may be employed for different cases (e.g. the relative lightness and chroma of the two cusp points), and the transformations may be non-linear, but usually all the points in the plane are governed by a single mapping formula. Such methods can result in unnecessarily large changes in the lightness of colours at the extremities of the lightness axis (notably in light yellow and dark blue-violet hues), and hence in significant changes to the overall image appearance.

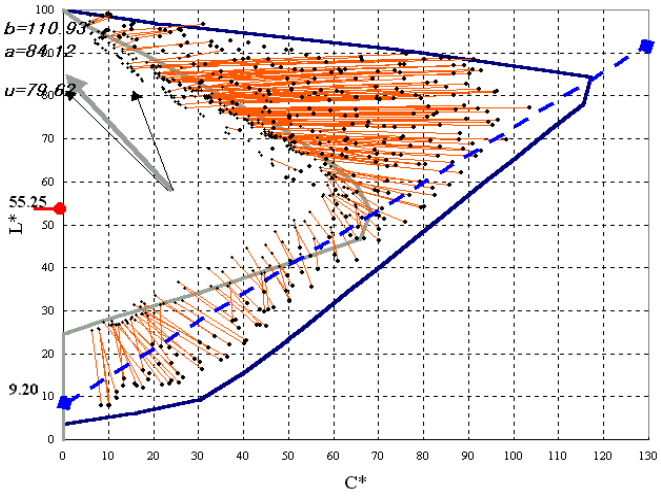

Figure 1. Gamut mapping from original (CRT, outside) to reproduction (ink-jet printer, inside) for hue angles in the range 128-180º (green). The dashed line passes through cusps of the two gamuts. (Reproduced by courtesy of B.H. Kang)

Recent investigation by Kang *et al.*[9] has produced some interesting insights into gamut mapping in general and gamut compression in particular. They asked observers to make interactive adjustments to an image to achieve the most satisfactory match to a simulated ink-jet print, adjacent on the CRT display. Observers were able to adjust lightness and chroma independently in three regions (high, medium and low) and hue in six regions (red, yellow, green, cyan, blue and magenta). The results indicate clearly the preferred translation vectors from original (CRT gamut) to reproduction (simulated print gamut), as shown in Figure 1 for the green hue angle.

Inspection of Figure 1 and of Kang's results for the other hues suggests the following aspects of observer preferences in gamut mapping:

1. The chords between corresponding colours in the original and destination are of lengths proportional to the local distance between the two gamut boundaries. The directions of the chords change as a function of lightness, but they do not converge to a single point. Instead they are approximately normal to the destination gamut boundary for dark colours (below the destination cusp), horizontal for lightnesses between the two cusps, and inclined at an angle for light colours (above the source cusp).
2. The colours within the reproduction gamut are largely untouched, but the mapping does extend a little inside the boundary, by about 10% at medium lightness values near the destination cusp. This suggests that the observers intuitively adopted a 'soft clipping' technique, in which chromatic gradations are preserved for colours near the gamut boundary while all other interior colours within a 'core gamut' are unchanged. Some variation in the thickness of the region between core and destination gamuts is evident when different hue angles are examined.

Description of the New Algorithm

A new gamut mapping algorithm is proposed, which transforms values from a source colour space into a destination colour space, preserving the relationships between source and destination in a reversible manner. The colour space is assumed to be perceptually uniform, with dimensions of hue, lightness and chroma. Hue angle is assumed to be invariant, so that the transformation maps pixel values within the lightness-chroma plane.

The algorithm is defined in four steps:

1) Construct the boundary of a 'core gamut', within which no colours are altered;
2) Define a distance metric along both source and core gamut boundaries;
3) Construct a set of mapping chords, connecting corresponding points;
4) Perform the gamut mapping along the chords, with a 'soft-clip' function.

Construct the Core Gamut Boundary

Let the source and destination gamuts be expressed in a plane of constant hue, as shown in Figure 2. Without loss of generality, assume that both source and destination gamuts are convex and that the source gamut lies entirely outside the destination gamut in the *L-C* plane. The maximum lightness of both gamuts is normalised to L_{max}=100.

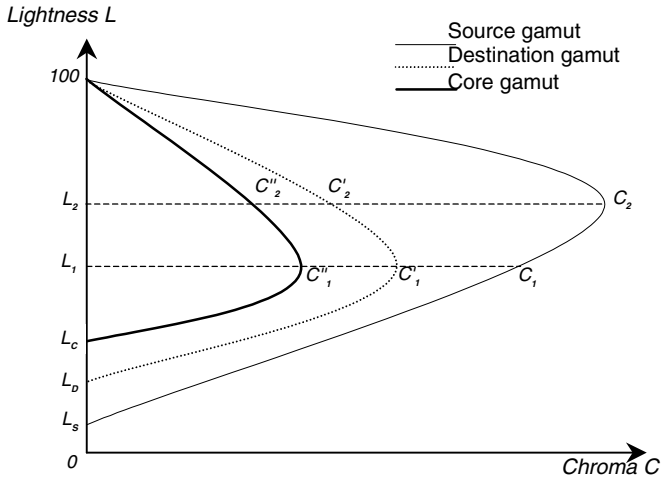

Figure 2. Gamut boundaries in the L-C plane.

Define the core gamut black point L_c to be greater than the destination gamut black point L_D by a factor •, of value typically in the range 1.2 to 1.5.

$$L_C = \alpha L_D \qquad (1)$$

Let L_1 be the lightness corresponding to the maximum chroma (or cusp) $C'_1 = max(C_D)$ of the destination gamut, and let L_2 be the lightness corresponding to the maximum chroma $C_2 = max(C_S)$ of the source gamut, as shown in Figure 2. Assume that $L_1 < L_2$.

Let the chroma of the destination gamut boundary be expressed as $C_D(L)$, a continuous single-valued function of L for $L_D \le L \le 100$. Then define the core gamut boundary $C_C(L)$ on the interval $L_C \le L \le 100$, such that the cusp $C''_1 = max(C_C)$ has the same lightness L_1 as that of the destination gamut:

$$\begin{aligned} C_C(L) &= \beta C_D(L) && for\ L_1 \le L \le 100 \\ C_C(L) &= \beta C_D(L_1 - \alpha(L_1 - L)) && for\ L_C \le L \le L_1 \end{aligned} \quad (2)$$

where β is a chroma-scaling constant, with typical value in the range 0.7 to 0.9, which may vary for different hue angles (see below). The core gamut and destination gamut are coterminous at the white point L=100.

Define a Distance Metric along Gamut Boundary

Define the parametric variable λ_S along the source gamut boundary on the interval $L_2 \le L \le 100$, i.e. the light tonal region:

$$\lambda_S = \frac{L - 100}{L_2 - 100} \quad (3)$$

Let the source gamut boundary be represented by a function $g_S(\lambda_S)$, $0 \le \lambda_S \le 1$, and define a distance metric d_S such that, for a small change $\Delta\lambda_S$ in parametric lightness, the corresponding change in distance along the source gamut boundary is:

$$d_S = \sqrt{\Delta\lambda_S{}^2 + (g_S(\lambda_S + \Delta\lambda_S) - g_S(\lambda_S))^2} \quad (4)$$

When the gamut boundary is represented as a series of n straight-line segments, connecting points g_{Si} (i=0..n) each change can be conveniently be calculated as the length of one segment. The total length of the source gamut boundary from L_2 to 100 is then:

$$D_S = \sum_1^n d_i = \sum_1^n \sqrt{(\lambda_{S_n} - \lambda_{S_{n-1}})^2 + (g_{S_n} - g_{S_{n-1}})^2} \quad (5)$$

Similar functions can be defined on the interval $L_S \le L \le L_1$, i.e. the dark tonal region, by defining the parametric variable:

$$\lambda_S = \frac{L - L_S}{L_1 - L_S} \quad (6)$$

Likewise define a distance metric d_C along the core gamut boundary on the interval $L_2 \le L \le 100$. For a small change $\Delta\lambda_C$ in lightness, the corresponding change in distance along the core gamut boundary is:

$$d_C = \sqrt{\Delta\lambda_C{}^2 + (g_C(\lambda_C + \Delta\lambda_C) - g_C(\lambda_C))^2} \quad (7)$$

When the gamut boundary is represented as a series of n straight-line segments, connecting points g_{Ci} (i=0..n) each change can be conveniently be calculated as the length of one segment. The total length of the core gamut boundary from L_2 to 100 is then:

$$D_C = \sum_1^n d_{Ci} = \sum_1^n \sqrt{(\lambda_{C_n} - \lambda_{C_{n-1}})^2 + (g_{C_n} - g_{C_{n-1}})^2} \quad (8)$$

Similar functions can be defined for the core gamut boundary on the interval $L_C \le L \le L_1$.

3.3 Construct the Mapping Chords

The *L-C* plane is divided into three regions, by range of lightness, as shown in Figure 3. The mapping chords, which define the local vector directions (or 'flow lines') of gamut mapping, are constructed separately in each region and generally have positive slopes in the upper region $L > L_2$, zero slope (horizontal) in the middle region $L_1 \le L \le L_2$, and negative slopes in the lower region $L < L_1$.

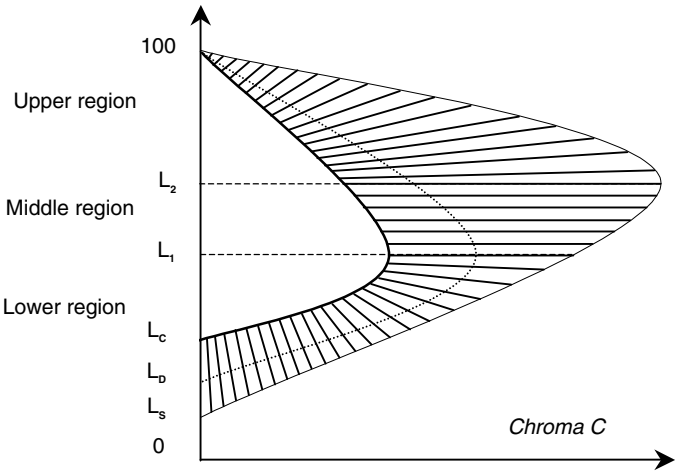

Figure 3. Chord directions in the three regions of gamut mapping.

In each region, locate n+1 points (L_{Si}, C_{Si}) for i = 0..n at equal intervals of length D_S/n along the source gamut boundary. Similarly, locate n+1 points (L_{Ci}, C_{Ci}) for i = 0..n at equal intervals of D_C/n along the core gamut boundary. Then construct n+1 chords connecting each (L_{Si}, C_{Si}) with the corresponding (L_{Ci}, C_{Ci}).

Perform the Gamut Mapping

A point P in the source gamut with co-ordinates (L, C) is to be mapped to a point P' in the destination gamut with co-ordinates (L', C'). The core gamut boundary represents the common sub-set of the two gamuts, within which no mapping occurs. Thus $P' = P$ for all points within the core gamut.

Points outside the boundary of the core gamut are mapped as shown in Figure 4 by the following procedure:

1. Find the two nearest chords on either side of P and, if not parallel, project them to intersect at X.

2. Construct a new chord from *X* through *P*, intersecting the source, destination and core gamut boundaries at P_S, P_D and P_C respectively.
3. In the case where the two chords are parallel, construct a new chord through *P* parallel to the other two.
4. Map *P* to *P′* using the bilinear 'soft clip' mapping function shown in Figure 5.

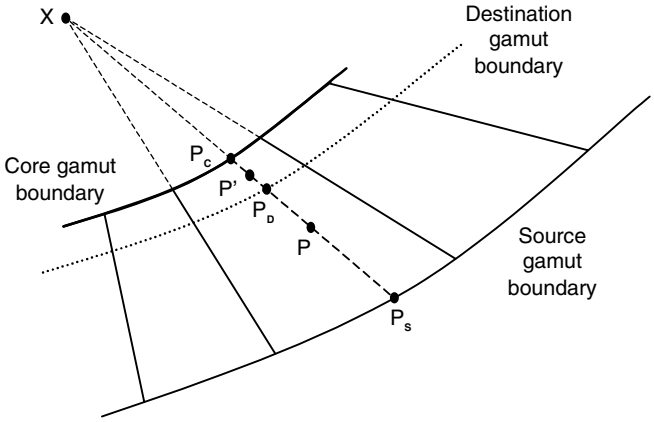

Figure 4. Construction of mapping chord.

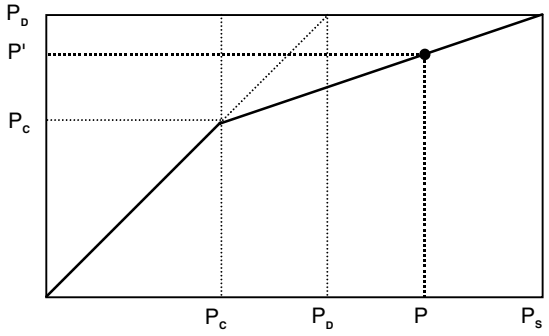

Figure 5. 'Soft-clip' gamut mapping function.

Discussion

The new algorithm is described as topographic because of the way it delineates and preserves the local features of the source and destination gamut boundaries. The objective is to map colours between corresponding points of the two gamuts, while preserving the rendering of gradations in lightness and chroma to the greatest degree possible. The technique is in some ways comparable to the mapping along curved lines proposed by Herzog and Büring[10] but is more closely attuned to the actual conformations of both source and destination gamut boundaries.

The concept of the 'core gamut' is not entirely new. Katoh and Ito proposed an 'onion-peel' method[11], in which an invariant 'colorimetric region' lies at the core of a series of 'virtual gamut boundaries'. This region was defined by scaling the destination (printer) gamut by a constant, the 'knee point' of the chroma compression function, and was coterminous with the destination gamut at both black and white points. Their results from experiments with four test images appeared to show a slight observer preference for a core gamut of scale 50%, although the trend was very dependent on image content. Sakamoto and Urabe also defined an 'original colour region' in a similar manner[12], but their compression knee point was determined by analysis of the chroma histogram.

The definition of the core gamut is critical to the effectiveness of the algorithm. We found in our initial trials that elevating the black point of the core gamut was important in preserving gradations in the shadow regions (dark tones) of the image. The region between the lower surfaces of the core and destination gamuts is where the dark colours are mapped from a source device having significantly lower black point than the destination device (as in Figure 1, for example). If this region is too narrow, as may happen when the core and destination gamut black points are coterminous, the shadow detail is greatly reduced or lost, and may result in contouring of the reproduced image.

The bilinear 'soft clip' function shown in Figure 4 preserves all colours unchanged within the core gamut, while mapping colours proportionally in the region between the core gamut and source gamut boundaries[11]. Values on the source gamut boundary are mapped onto the destination gamut boundary. The linear 1:1 mapping preserves the relationships between values and is thus invertible, subject to the quantising of the image coding.

The new algorithm assumes that the source and destination gamut boundaries are known *a priori*, and that they can be accurately represented at each hue angle. Each gamut boundary should be well-behaved, i.e. chroma *C* expressible as a smooth and continuous single-valued function of lightness *L*. Implementation should account for cases where the maximum chroma of the source gamut occurs at higher, equal and lower values of lightness than the maximum chroma of the destination gamut.

The algorithm should also perform well for cases where the destination gamut is larger than the source gamut, i.e. gamut expansion rather than gamut compression, and for mixed cases where the gamut boundaries cross over, so that gamut expansion is required in some regions and gamut compression in others.

Evaluation of Performance

Implementation of Algorithm

The topographic gamut mapping algorithm (TOPO) was implemented in the ANSI C language in the Microsoft Visual C++ programming environment. Images were converted into the CAM97s2 colour space,[13] and the gamut mapping performed in the perceptual dimensions of lightness (*J*) and chroma (*C*). The source device was a Barco *Calibrator V* monitor, characterised by the Berns GOG model.[14] The reproduction device was a Hewlett Packard 895c ink-jet printer, characterised by fitting third-

order polynomials to colorimetric densities measured from 9x9x9 printed colour patches[15]. Device gamut boundaries were described using the Flexible Sequential Line Gamut Boundary (FSLGB) method developed by Morovic.[1]

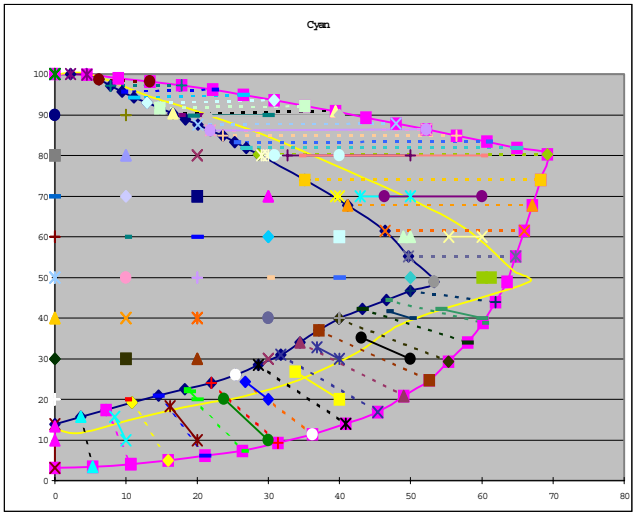

Figure 6. Validation of TOPO algorithm for cyan hue angle.

The parameters α and β used in the construction of the TOPO core gamut (Eq. 1 and 2) were set to constant values α = 1.2 and β = 0.8. The gamut boundary descriptors were calculated for 1° intervals of hue angle. The implementation of TOPO was validated by plotting the mapping chords for various hue angles, as shown in Figure 6. The dashed lines are chords constructed between corresponding points on the source and core gamut boundaries. Points inside the core gamut remained unchanged, while points in the region between the core and source gamut boundaries were mapped along the calculated chord directions into the region between the core and destination gamut boundaries.

For comparison of the performance of the TOPO algorithm, three other algorithms used in the previous study[1] were also applied to each test image, using the same gamut boundary data:

MDE	Minimum ΔE clipping to gamut boundary, preserving hue (in L-C plane).
LLIN	Linear compression of lightness and chroma.
GCUSP	Chroma-dependent lightness compression and linear compression to cusp.

Experimental Design

The performance of the new algorithm was evaluated using the same experimental technique and test images employed previously by Morovic and Luo,[1] in order to permit the direct comparison of results. The images were simultaneously viewed side-by-side, with the source image displayed on the CRT and two reproduction prints in a Verivide viewing booth under a simulated D65 light source, meeting the ISO 3664 viewing condition P2. Both the white point and the grey background on the CRT were carefully matched to the corresponding colours in the booth, based on spectroradiometric measurement. The images subtended equal visual angles to the observer, viewed from a distance of approximately 80 cm. Other conditions were as described in the evaluation guidelines under development for CIE TC8-03.[16]

Five test images were chosen to contain a range of different types of pictorial content and tonal and chromatic variety, as shown in Figure 7. Twenty prints were produced (5 images times 4 algorithms). Twelve observers, all students and staff of the Colour & Imaging Institute with normal colour vision and ages ranging from 20 to 38, took part in the experiment. Each observer was therefore required to make ${}^4C_2$=6 pair-wise comparisons per image, a total of 30 comparisons per session. The observer's task was to decide which of the two prints in the viewing booth was the better overall match to the original (source) image displayed on the CRT.

Figure 7. The five test images: MUS, SKI, GIRL, NAT, BUS

Results

For each image, the 4x4 matrices of comparison results for each observer were averaged over the 12 observers and transformed into z-scores. Results are given in Table 1 and the overall z-scores for the four algorithms are plotted in Figure 8.

Table 1. Z-scores from pair comparison experiment for each image and algorithm.

	TOPO	GCUSP	MDE	LLIN	Stdev
MUS	2.17	0.41	-1.36	-1.22	1.66
SKI	0.82	2.44	-2.18	1.72	2.03
GIRL	0.97	-0.67	2.61	-2.90	2.35
NAT	-1.68	2.30	-1.74	1.12	2.03
BUS	-1.82	3.66	0.55	-2.40	2.75
Overall	0.09	1.63	-0.42	-0.73	1.05

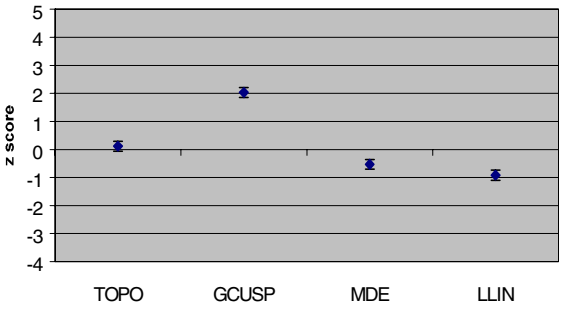

Figure 8. Overall z-scores for the four algorithms.

Table 2 gives the ranking of the performance of the four algorithms for the five test images. GCUSP was best overall and TOPO second best. TOPO was ranked highest for the MUS image, in which it preserved the lightness rendering better than the other algorithms, especially in the skin colours.

Table 2. Ranking of algorithm performance vs image (1=best, 4=worst)

	GCUSP	TOPO	MDE	LLIN
BUS	1	3	2	4
MUS	2	1	3	3
GIRL	3	2	1	4
NAT	1	3	3	2
SKI	1	2	4	3
Overall	1	2	3	4

TOPO performed poorly for the NAT image, because observers judged the blue sky to be too dark, and also for the BUS image, because the loss in chroma was too great. Curiously, the MDE algorithm was ranked best for the GIRL image because it had little effect on the skin colours, which were largely inside the printer gamut boundary.

Conclusions

In summary, it was found that the TOPO algorithm produced good visual results for images of high tonal contrast in which the proportion of high-chroma colours outside the destination gamut was not too large. Its performance for high chroma blue colours was poor, possibly due to a problem with the characterisation of the printer. Its performance for images containing large areas of colours of maximum chroma, such as the business graphics image, was also poor because the mapping chords for medium to high lightness were close to horizontal, resulting in substantial reduction in the chroma of the reproduction.

Nevertheless, we believe that the TOPO algorithm has great potential for further refinement in the following ways:

- Definition of the core gamut, adapting to the relative sizes and shapes of both source and destination gamut boundaries and lowering the white point of the core gamut to create a mapping region for light colours;
- Introduce a non-linear (perhaps quadratic) soft-clip function, instead of the bilinear function, to give increased chroma for the reproduction of out-of-gamut source colours;
- Reduce the number of regions in the *L-C* plane from three to two, above and below the lightness of the core gamut cusp, which in general may differ from the lightness of the destination gamut cusp;

We are planning further development of the TOPO algorithm and will test it with: (1) more test images; (2) more algorithms; (3) simulated prints on the display; (4) prints on a commercial printing press; and (5) experiments in which observers judge the reproduction quality in individual regions of colour space.

References

1. J. Morovic and M.R. Luo, Developing Algorithms for Universal Colour Gamut Mapping, *Colour Imaging: Vision and Technology*, Ed. L.W. MacDonald and M.R. Luo, John Wiley & Sons, pp. 253-282 (1999)
2. K.M. Braun, R. Balasubramanian and R. Eschbach, Development and Evaluation of Six Gamut-Mapping Algorithms for Pictorial Images, *Proc. IS&T/SID Seventh Color Imaging Conf.*, pp. 144-148 (1999)
3. L.W. MacDonald and J. Morovic, Assessing the Effect of Gamut Compression in the Reproduction of Fine Art Paintings, *Proc. IS&T/SID Third Color Imaging Conf.*, pp. 194-200 (1995)
4. J. Morovic and P.L. Sun, Methods for Investigating the Influence of Image Characteristics on Gamut Mapping, *Proc. IS&T/SID Seventh Color Imaging Conf.*, pp. 138-143 (1999)
5. L.W. MacDonald, Gamut Mapping in Perceptual Colour Space, *Proc. IS&T/SID First Color Imaging Conf.*, pp. 193-196 (1993)
6. A.J. Johnson *et al.*, Colour Appearance Research for Interactive System Management and Applications (CARISMA), *Report WP2-19 Colour Gamut Compression* (1992)
7. P.J. Green and M.R. Luo, Developing the CARISMA Gamut Mapping Model, *Proc. Colour Image Science 2000*, University of Derby (2000)
8. E. Pirrotta, T. Newman and L. Lavendel, a "Universal" Gamut Mapping Algorithm?, *Proc. Colour Image Science 2000*, University of Derby (2000)
9. B.H. Kang, M.S. Cho, J. Morovic and M.R. Luo, Gamut Compression Algorithm Development Using Observer Experimental Data, *Proc. Colour Image Science 2000*, University of Derby (2000)
10. P.G. Herzog and H. Büring, Optimizing Gamut Mapping: Lightness and Hue Adjustments, *Proc. IS&T/SID Seventh Color Imaging Conf.*, pp. 160-166 (1999)
11. N. Katoh and M. Ito, Applying Non-linear Compression to the Three-Dimensional Gamut Mapping, *Proc. IS&T/SID Seventh Color Imaging Conf.*, pp. 155-159 (1999)

12. K. Sakamoto and H. Urabe, Development of XYZ/sRGB-SCID and Color Gamut Compression, *Proc. IS&T/SID Seventh Color Imaging Conf.*, pp. 212-216 (1999)
13. C. Li, M.R. Luo and R.W.G. Hunt, The CAM97s2 model, *Proc. IS&T/SID Seventh Color Imaging Conf.*, pp. 262-263 (1999)
14. R.S. Berns, Methods for characterizing CRT displays, *Displays*, **16**, 4, pp. 173-182 (1996)
15. T. Johnson, Methods for characterizing colour printers, *Displays*, **16**, 4, pp. 193-202 (1996)
16. http://www.colour.org/tc8-03/